HHS Public Access

Author manuscript

Arch Biochem Biophys. Author manuscript; available in PMC 2019 June 01.

Published in final edited form as:

Arch Biochem Biophys. 2018 June 01; 647: 84–92. doi:10.1016/j.abb.2018.04.002.

HCM and DCM cardiomyopathy-linked α-tropomyosin mutations influence off-state stability and crossbridge interaction on thin filaments

Gerrie P. Farman[1,2,*,#], **Michael J. Rynkiewicz**[2,#], **Marek Orzechowski**[2,+], **William Lehman**[2], and **Jeffrey R. Moore**[1]

[1]Department of Biological Sciences, University of Massachusetts-Lowell, One University Avenue, Lowell, MA 01854, USA

[2]Department of Physiology & Biophysics, Boston University School of Medicine, 700 Albany Street, Boston, MA 02118, USA

Abstract

Calcium regulation of cardiac muscle contraction is controlled by the thin-filament proteins troponin and tropomyosin bound to actin. In the absence of calcium, troponin-tropomyosin inhibits myosin-interactions on actin and induces muscle relaxation, whereas the addition of calcium relieves the inhibitory constraint to initiate contraction. Many mutations in thin filament proteins linked to cardiomyopathy appear to disrupt this regulatory switching. Here, we tested perturbations caused by mutant tropomyosins (E40K, DCM; and E62Q, HCM) on intra-filament interactions affecting acto-myosin interactions including those induced further by myosin association. Comparison of wild-type and mutant human α-tropomyosin (Tpm1.1) behavior was carried out using *in vitro* motility assays and molecular dynamics simulations. Our results show that E62Q tropomyosin destabilizes thin filament off-state function by increasing calcium-sensitivity, but without apparent affect on global tropomyosin structure by modifying coiled-coil rigidity. In contrast, the E40K mutant tropomyosin appears to stabilize the off-state, demonstrates increased tropomyosin flexibility, while also decreasing calcium-sensitivity. In addition, the E40K mutation reduces thin filament velocity at low myosin concentration while the E62Q mutant tropomyosin increases velocity. Corresponding molecular dynamics simulations indicate specific residue interactions that are likely to redefine underlying molecular regulatory mechanisms, which we propose explain the altered contractility evoked by the disease-causing mutations.

Corresponding author: Jeffrey R. Moore, Jeffrey_Moore@uml.edu.

[*]Current address: Department of Cellular & Molecular Medicine, University of Arizona, 1656 E. Mabel Street, Tucson AZ 85719, USA.

[+]Current address: Broad Institute, 415 Main Street, Cambridge MA 02142, USA.

[#]Contributed equally to this study.

Author contributions

All authors participated in formulating the work performed in this study and in analyzing the data produced. G.P.F. performed the *in vitro* motility assays. M.J.R. and M.O. carried out MD. J.R.M. and W.L. wrote the manuscript.

Keywords

in vitro motility; tropomyosin; cardiomyopathy; muscle regulation; molecular dynamics simulations

Introduction

Tropomyosin is a coiled-coil protein that binds along the long-pitch helix of actin. Tropomyosin, in concert with the troponin complex, inhibits myosin-binding, which leads to inhibition of striated muscle contraction that causes muscle relaxation. To explain the kinetics of this process, McKillop and Geeves [1,2] introduced a three-state kinetic model for thin filament activity and its regulation, describing blocked, closed and open states, where only the open-state is fully activated, the blocked-state is fully inhibited and the closed-state represents an intermediate off-state between the two end states. Subsequent support for the kinetic scheme came with structural evidence [3], showing that tropomyosin alternates between occupying one or another of three defined positions on the actin filament, *viz*. B-, C- and M-states. Here, the three structural states display different levels of obstruction and exposure of the myosin-binding site on actin, depending on calcium binding to troponin and myosin-binding on actin. In each of these schemes, tropomyosin acts as an inhibitor in two of these states (blocked/B and closed/C), absent myosin interactions, with the blocked/B-state being stabilized by the calcium-free troponin complex [4–7]. The probability of tropomyosin occupying either of the two off-states depends on a number of factors in addition to cytosolic calcium concentration altering troponin conformation. For example, ionic strength, pH, isoform [8], stretch [9] as well as a variety of mutations, may alter tropomyosin affinity for, or position on, actin [10].

Thin filaments examined structurally at low intracellular levels of calcium reveal that tropomyosin, in fact, is constrained toward the outer domain of successive actin molecules blocking myosin-binding sites along thin filaments (the B-state position). Calcium-binding to the TnC-subunit of troponin induces a conformational change in the entire troponin complex that promotes tropomyosin movement toward the inner domain of actin (the C-state position). This transition, while still in an off-state, partially frees the “closed” myosin-binding site and facilitates weak non-force producing myosin-interaction, which then likely auto-induces even further tropomyosin movement to an open M-state position and leads to full muscle activation [3,11]. The correspondence between steps in the structural and kinetic descriptions suggest that they are manifestations of the same process.

Molecular dynamics simulations guided by reconstructions of muscle thin filament electron micrographs reveal that each tropomyosin molecule interacts with seven consecutive actin monomers by means of a locally repeating pattern of weak electrostatic interactions [12,13]. Energy landscape calculations [14,15] additionally show that tropomyosin position on actin is determined by a shallow interaction-potential well close to its corresponding location in the low-calcium blocked/B-state [14–16]. Absent myosin, the electrostatic interaction energy between actin and tropomyosin is significantly weaker in the open/M-state [15,16]; however, binding is typically robust in the open/M-state because, in addition to interacting with actin,

tropomyosin is normally trapped topologically on actin in a binding channel formed by the inner edges of actin and the bound myosin-head [17]. Thus, disease-linked mutations that either weaken or strengthen interactions between actin and tropomyosin in the blocked/B-state or those flanked by myosin in the open/M-state will inevitably affect actomyosin interactions and hence, in distinct ways, contractility.

Our objective is to determine the effects of the mutations on actin-tropomyosin interactions and their impact on strong-binding of myosin cross-bridge formation during activation of contractility. We approach this objective by studying the performance of reconstituted thin filaments containing wild-type and a variety of disease-causing mutant tropomyosins. In the current work, we investigated two mutations, where based on energy landscape determination one has been predicted to effectively stabilize (E40K tropomyosin) and the other to strongly destabilize (E62Q tropomyosin) blocked/B-state thin filaments [14]. Indeed, we find that these mutations disrupt the regulatory switching mechanism in markedly distinct ways, in one case leading to decreased and in the other increased calcium-sensitivity of thin filament activation. The E40K point mutation occurs at an "*e*-heptad position" [18], normally participating in "*e*-*g*" pairing. *e*-*g* pairs in coiled-coils such as tropomyosin form an electrostatic ridge linking component chains of the dimer together while shielding hydrophobic, *a* and *d*, core residues from solvent (Fig. 1A) [19]. In contrast, the E62Q mutation occurs at an *f*-heptad position [20], which would be solvent exposed in the canonical heptad repeat and in a position frequently engaged in tropomyosin-actin interaction. Thus, the effect of this mutation is likely to differ markedly from that of E40K (Fig. 1B, C). Indeed, in the current study, myosin-dependent *in vitro* motility of actin filaments (in the presence and absence of troponin) showed reduced velocity when E40K tropomyosin was included in assays and conversely increased velocity when E62Q was added. These results are suggestive of an E40K mutation-induced stabilization of the tropomyosin in the blocked/B-state, and alternatively a destabilization by E62Q, as implied by prior energetics [14] and now corroborated by molecular dynamics measurements in the current work. Our computational analysis indicates that local and long-range alterations in tropomyosin conformation and in tropomyosin-actin interactions appear to underlie the altered regulatory switching. Our new data highlight likely residue-level specific perturbations, which translate into distinct disease-causing mechanisms, namely they suggest how two tropomyosin mutations influence blocked/B-state binding stability in different ways. In addition, the functional effects noted here cannot simply be based on changes in tropomyosin coiled-coil flexibility, frequently invoked to describe the action of tropomyosin mutations without convincing direct support.

Methods and Materials

Molecular Dynamics

Molecular dynamics was performed on isolated tropomyosin as detailed by Li et al. [21] and on the actin-tropomyosin complex as described previously [13]. In the latter case, a model of two tropomyosin coiled-coil dimers extending from either side of an overlapping domain on F-actin was represented by tropomyosin residues 134-1 on the N-terminal side of the overlap nexus linked to residues 284-234 on the C-terminal side, while the tropomyosin model

associated with five actin subunits [13]. The mutations at positions 40 and 62 incorporated into this model are located in the middle of the structure used. Amino acid substitutions to characterize mutant tropomyosins were made in VMD [22] and 30 ns of MD of the acto-tropomyosin model in explicit solvent was carried out at 300 K as previously using the program NAMD [23]. The average structure throughout MD was calculated in CHARMM [24]. The frame of MD closest to average structures determined by its low Root Mean Square Deviation (RMSD) to backbone atoms was used for display in Figure 2.

The persistence length and local flexibility (δ) of isolated tropomyosin (i.e. free of actin) was assessed over the last 10 ns of a 30 ns MD calculation as in Li et al. [21,25]. Here, CHARMM was used for MD [24] performed in implicit solvent. The apparent persistence length (PL_a) was calculated by the tangent correlation method as previously described [21,25], using the relationship $\langle\cos(\theta[s(t)])\rangle_{s(t)}=\exp[-s/PL_a]$, where s is a segment of increasing arc length (of up to 300 Å) over which $\theta[s(t)]$ was measured at times t of the MD simulation. PL_a is a measure of deviations of tropomyosin from a notional straight rod.

The local bending flexibility of tropomyosin (δ) was measured over the last 10 ns of simulation by taking each tropomyosin snapshot from MD trajectory files and dividing the individual tropomyosin conformers into overlapping segments consisting of nine successive residues acquired along the entire length of the molecule (i.e. residues $i - i+9$, $i+1 - i+10$, $i+2 – i+11$, $i+3 – i+12$, … $i + 275 - i+284$). Each separate segment was centered on and fitted to corresponding residues in the time-averaged tropomyosin structure and angular deviation between that segment and the average structure was calculated (i.e. the tangent of the segment to the super-helical average was quantified). The mean deviation determined at any position along tropomyosin during the 10 ns period defined the local δ [21,25].

The dynamic persistence length (PL_d), a test of the overall flexibility of a curved rod-like tropomyosin, was calculated from an average of all local delta values using the equation $\cos\langle\delta\rangle=\exp[-s/P_d]$, where s, the nine residue segment, for each local delta value was 14.4 Å. These methods and corresponding algorithms are detailed previously [21,25].

DNA Construction and Protein Purification

Mutagenesis of wild-type human striated α-tropomyosin (Tpm1.1), containing the N-terminal extension Met-Ala-Ser, was detailed previously [14]. E40K mutant tropomyosin was generated by similar methods but with the primer pair: 5′ **A**GATGAGCTGGTTAGCCTGCAG 3′ (FORWARD PRIMER) 5′ **TT**CAGCTGCTTGCTACGATCCTC 3′ (REVERSE PRIMER). Mutant tropomyosin was prepared as described in [26].

Tropomyosin Binding and Reconstitution of Thin Filaments

To determine the apparent affinities of our tropomyosin variants for actin we performed co-sedimentation experiments with F-actin. In these experiments 7 μM F-actin was mixed with various amounts of human recombinant tropomyosin containing met-ala-ser and either the E40K mutation, E62Q mutation, or Wild-Type sequences. F-actin and tropomyosin were combined and incubated for 30 minutes. Tropomyosin bound to F-actin was isolated by

centrifugation at 100,000 g, in an Airfuge (Beckman-Coutler) for 30 minutes. The resulting supernatant was then removed and the pellet was washed with a low salt solution to remove unbound proteins. The pellet was solubilized in an equal volume of gel running buffer containing 6M Urea and 10 mM β-mercaptoethanol and tropomyosin bound to F-actin was then determined via SDS-PAGE. Gels were stained with Coomassie Blue and bands corresponding to tropomyosin and actin were quantified via densitometry and ImageJ analysis. The amount of tropomyosin bound to actin was determined by first normalizing the actin in each lane to the total amount of actin used in the experiment. Then the amounts of tropomyosin were scaled to these new values and plotted versus the amount of free tropomyosin added to the solution. The resulting data were fit to a Hill-type cooperative binding model $Y=B_{max}*[Tm]^h/(Kd^h + [Tm]^h)$ using GraphPad Prism 7.04 Software to determine apparent affinity and binding cooperativity.

Actin filaments were reconstituted for *in vitro* motility assays by incubating TRITC labeled actin (1 μM) with either wild-type, E40K, or E62Q tropomyosin (0.6 μM) overnight at 4°C. For experiments involving fully regulated thin filaments, human recombinant cardiac troponin complex (0.6 μM) was incubated with actin-tropomyosin for at least one hour. Reconstituted thin filaments were stored at 4 °C and used within five days.

Calcium-Regulated Motility

In vitro motility assays were performed with porcine skeletal muscle myosin and porcine cardiac actin at 30 °C as described previously [14] with solutions prepared as described [14]. Prior to addition to the flow cell assay chamber, the reconstituted thin filaments were diluted 1:200 in actin buffer containing HDTA, instead of EGTA, to remove any potential for residual EGTA in the flow cell prior to addition of motility buffer at the desired pCa to the flow cell [27]. The reconstituted thin filaments were incubated with surface-bound myosin for three minutes followed by another three-minute incubation of 300 nM troponin/ tropomyosin to insure binding of regulatory proteins. Motility was induced by the addition of motility buffer containing 1 mM ATP at various pCa levels from pCa 10 to 4.

Myosin-dependent activation

To examine how tropomyosin mutations impact myosin-activated thin filament motility, we measured actin sliding velocity as a function of increasing myosin concentration. In this assay, actin filaments, either fully-regulated with troponin and tropomyosin or complexed with just tropomyosin, translocate at maximum velocity if, at all times during filament movement, at least one myosin head is interacting with the actin filament. The probability of strong cross-bridge formation is related to (1) the number of available myosin heads (loading concentration, ρ) and target sites, which is in part controlled by the activity of the tropomyosin, and (2) the fraction of time that the myosin molecule remains bound r (duty cycle). Thus, the probability that at least one head is interacting with actin at all times is given by the statement $1-(1-r)^\rho$. Therefore, velocity will be altered as a function of r and ρ according to the equation: $V_{obs}= V_{max}[1-(1-r)^\rho]$ where V_{obs} is the observed velocity of the actin filament and V_{max} is the maximal sliding velocity at saturating myosin concentrations [28,29].

Statistics

Standard tests of significance and of significant differences of points in plots measuring filament motility were done by comparing standard errors, where minimum p-values less than 0.05 were considered significant. Hill curves were plotted and Hill coefficients (n_H) calculated by fitting velocity data (V) versus calcium concentration according to the equation:

$$V = \frac{V_{max}[Ca^{2+}]^{n_H}}{pCa_{50} + [Ca^{2+}]^{n_H}}$$

Tests of significance of Hill coefficients were performed using the “compare function” in the program Prism (GraphPad 7825, La Jolla, CA 92037 USA). Here, significance and significant differences between plotted curves was determined by an extra sum-of squares F-test where differences between wild-type and mutant curves with p-value less than 0.05 were considered significant.

Results

Molecular Dynamics of Mutant and Wild-Type Tropomyosin

In order to examine the impact of the E40K and E62Q mutations on the structure of, and interactions between, tropomyosin and actin, we performed molecular dynamics simulations of wild-type and mutant tropomyosin on actin, as described in the Materials and Methods and previously [13]. Figure 2 shows that the introduction of either the DCM mutant, E40K (Fig. 2C) or HCM mutant, E62Q, (Fig. 2D) alters the interactions of tropomyosin side chains and actin. In the case of the E40K mutant, a number of negatively charged residues on actin could potentially interact favorably with the mutant lysine side chain; however, most of these are too distant from the mutant side chain to have a significant effect. The closest of these on actin, E93 and E334, have a minimum distance of 8.2 Å and 7.3 Å to the mutant K40 tropomyosin side chain during the MD simulations, suggesting a small impact to tropomyosin-actin association. In contrast however, side chain interactions within the tropomyosin molecule itself are affected by the mutation. While side chains at *e*-position E40 and *g*-position R35 form stereotypical (*i,i+5*) inter-chain *e-g* pair (Fig. 2A), salt bridges in the crystal structure [19] and in MD models of wild-type tropomyosin, mutant K40 and R35 do not (Fig. 2C). Thus, introducing the DCM-associated mutation, E40K, makes this interaction unfavorable by replacing the negatively charged glutamic acid with a positively charged lysine side chain. During the simulation, the loss of the salt bridge between E40 and R35 is compensated by a new inter-chain salt bridge formed between the side chains of tropomyosin R35 and *e*-position E33 (Fig. 2C). This rearrangement (see Fig. 1D) is noted at the beginning of the MD production runs of both actin-tropomyosin in explicit solvent and isolated tropomyosin in implicit solvent. In both cases, the alteration is constant throughout simulation (see Supplementary Item 1). Moreover, the effect can be propagated locally resulting in changed inter-chain pairing in N- and C-terminal directions accompanied by new K40-E42 side chain orientation and altered E-33-K29-D28,E26 bonding. This side

chain redistribution in the mutant is likely to affect the structure-function relationships of the tropomyosin coiled-coil (Fig. 2E), creating further alterations in the actin-binding residues C-terminal to the mutation site. In particular, tropomyosin residue S45 is shifted in relation to the actin filament, forming a novel hydrogen bond interaction between E40K tropomyosin and the side chain of R28 of actin. Consistent with previous energy landscape determinations [14], these new interactions are expected to increase the affinity of the E40K mutant tropomyosin for actin. Therefore, evidently more energy will be required to move the mutant from the B-state position during regulatory transitions on the thin filament.

Based on previous work [14], HCM mutant E62Q, unlike E40K, is predicted to have a lower affinity for the B-state position on actin. In the wild-type model, the E62 side chain is positioned to make salt bridge interactions with two positively charged side chains on actin, R147 and K328 (Fig. 2B). Although mutation of E62 to glutamine is relatively conservative, the amide side chain of the glutamine cannot form an ionic bridge with the two positively charged residues on actin. In the simulations, the loss of the negative charge on tropomyosin results in loss of interaction between Q62 of tropomyosin with actin residues R147 and K328 (Fig. 2D). This divergence from the wild-type model also occurs at the beginning of the MD production run and is stable throughout simulation (Supplementary Item 2). Moreover, additional reduction in affinity is expected from the movement of the tropomyosin coiled-coil away from the actin surface in the simulation (Fig. 2F), also affecting interaction strength in the vicinity of the mutation, even though there was no apparent concomitant mutation-induced change in coiled-coil flexibility or overall equilibrium binding of E62Q mutant tropomyosin binding with actin (see below; Fig. 3 and 4). Thus, the E62Q mutation is expected to have a lower local affinity for actin than that for the wild-type, and thus would require less energy to move from the B-state to the C- and M-states.

Mutant tropomyosin flexibility

The semi-rigidity of tropomyosin contributes to tropomyosin’s cooperative motions on actin filaments and hence its regulatory position [21]. Typically stiffness or flexibility of an object is defined by its flexural and torsional mobility as well as its linear elasticity. Here, flexural variance of the tropomyosin mutants was measured during MD, namely we quantified the extent of their bending fluctuations and compared the data to that of the wild-type tropomyosin. To determine overall tropomyosin flexibility, we assessed persistence length, a measure of thermal bending variance (Table 1). Persistence length measurements of rod-like structures like tropomyosin determine the aggregate bending fluctuations about that structure and thus reflects the material properties of the molecule. In order to best assess material properties of tropomyosin in a simple and meaningful fashion, isolated tropomyosin molecules were examined, unconstrained by extra-molecular interaction. In contrast, once bound to actin, tropomyosin’s inherent bending fluctuations will be curbed by head-to-tail polymerization, limited by the topological organization of tropomyosin on the F-actin helix, and dampened further by electrostatic interactions with the actin substrate, where its bending may be dominated by motions of the actin filament and not by tropomyosin’s intrinsic molecular flexibility.

The structure of actin-free tropomyosin is characteristically curved. Indeed, to a varying extent tropomyosin is pre-shaped to match to the helical pitch of F-actin [21,30]. This innate curvature of tropomyosin spuriously contributes to standard calculation of persistence length, usually measured against uniformly straight reference structures. Tropomyosin's bending deviations from such an idealized straight rod yields a so-called "apparent" persistence length (PL_a) (approximately 90 to 130 nm), which over-estimates flexibility. We therefore determined a "dynamic" persistence length, PL_d, the true measurement of flexural stiffness that accounts for the average curvature of the molecule (see Materials and Methods section). We accomplished this by measuring flexural deviations from tropomyosin's average curved shape [21,25]. Our results show that the E62Q mutation does not affect tropomyosin flexibility. However, E40K is more flexible and, on average, straighter than the wild-type (Table 1).

As mentioned, persistence length measures the aggregate flexural rigidity of rod-like structures and is most useful for assessing isomorphous materials. However, the amino acid sequences of each tropomyosin actin-binding pseudo-repeat differ (see Fig. 1) and hence tropomyosin flexibility is not uniform along its length [21,25]. Thus, local alteration in curvature and bending dynamics along the tropomyosin coiled-coil may also be mutation specific. We therefore also assessed the effects of the disease-linked mutations on local tropomyosin flexibility. For these measurements, we determined the bending variance (local δ) one residue at a time over all tropomyosin residues during the entire course of simulation relative to residues in the average structure. The local delta angle provides a measure of tropomyosin super-helical flexibility, where a larger angle reflects greater deviation from the average for that residue during the simulation and therefore indicates greater local flexibility. As expected, the E40K mutation alters tropomyosin local flexibility near to the site of the mutation (Fig. 3) where the changed *e-g* pairs have realigned, and this change in flexibility is stable over time (Supplementary Item 3). The local effect apparently is propagated toward the N-terminus of the mutant structure (Fig. 3). In addition to the localized effects observed, the simulations also show that the E40K mutation has prominent delocalized effects toward the C-terminus, where *a* and *d* heptad positions are less frequently occupied by canonical Leu, Ile, or Val residues and *e-g* pairing is irregular. The alterations in tropomyosin flexibility and shape parallel the changed pattern of tropomyosin-actin interactions observed in MD of E40K on actin (Fig. 2). In contrast, measurements of E62Q tropomyosin persistence length and local delta show that, unlike E40K tropomyosin, both the tropomyosin E62Q local and aggregate flexibility is similar to wild-type (Fig. 3, Supplementary Item 3). This is expected since residue 62 occupies an *f*-heptad position, *viz.* it protrudes orthogonally from the tropomyosin coiled-coil and apparently is not required for coiled-coil rod-stability, but instead is involved in actin interaction [12].

Altered local affinity of mutant tropomyosins interfere with myosin-driven thin filament motion

Mutant tropomyosin molecules were expressed in E.coli and purified as described previously [14]. Mutant tropomyosin interaction with F-actin was assessed via SDS-PAGE and cosedimentation as described previously [31]. Despite the altered actin-tropomyosin interactions propagated by the tropomyosin mutations and observed via MD simulations, no

obvious differences in apparent affinity values were found for F-actin and mutant tropomyosin versus those for F-actin and wild-type tropomyosin (Fig. 4). Thus, equilibrium binding and the formation of the tropomyosin polymer on actin appear to be unaffected by these tropomyosin mutations.

To determine other possible functional effects of the altered tropomyosin-tropomyosin and tropomyosin-actin interactions revealed by the MD simulations, we evaluated the cooperative activation of thin filaments containing mutant and wild-type tropomyosins in the absence of troponin (Fig. 5). Using an *in vitro* motility assay, we measured the impact of the tropomyosin mutations analyzed above on actin sliding velocity and on the fraction of regulated filaments that were motile. At the low concentrations employed in the motility assay, the presence of wild-type tropomyosin decreased maximal velocity when compared to that of tropomyosin-free actin controls, a phenomenon well described by others [32]; nonetheless, the presence of E62Q tropomyosin was not inhibitory, consistent with destabilization of the B-state positioning observed structurally.

Compared to the motility of control tropomyosin-free F-actin, more myosin was required to maximally stimulate actin-tropomyosin-based motility judging from corresponding plots of the fraction of filaments which were motile (fraction “%” motile) (regardless of the presence or type of mutant or wild-type tropomyosin). In contrast, thin filaments containing E40K tropomyosin required a similar amount of myosin to reach maximal activation, while filaments containing wild-type E62Q-mutant tropomyosin reached maximal velocity at lower concentrations (Figure 5B), again consistent with destabilization of the B-state by the E62Q tropomyosin mutation (Fig. 1).

Velocity/pCa Relationship

To test if weakening or enhancing the interaction between tropomyosin and actin alters calcium-regulated actomyosin activity, we again measured the impact of the two tropomyosin mutations on actin sliding velocity and the fraction of regulated filaments motile for filaments now containing both tropomyosin and troponin. As shown in Figure 6, wild-type tropomyosin/troponin fully inhibited thin filament motility at low calcium concentrations and, as calcium concentration was increased, actin filament movement increased cooperatively over a narrow pCa range. Compared to wild-type, troponin-tropomyosin regulated actin filaments containing the HCM mutant E62Q activated at lower calcium (i.e. they were sensitized) when assessed either by sliding velocity or by fraction motile. Conversely, actin filaments containing the DCM mutant E40K required higher calcium to maximally activate sliding velocity and fraction motile (i.e. they were desensitized) (Fig. 6, Table 2).

Interestingly in the case of the E62Q mutant, the Hill-Coefficient for the actin sliding velocity relationship was lower than that for wild-type; however, fraction motile values were in fact not very different from each other. In contrast, the Hill-Coefficient for the E40K mutant was lower for both the measured fraction motile and sliding velocity. A slightly reduced maximal filament sliding speed was also observed for E40K.

Myosin-dependent activation

Strong binding of myosin to actin during the closed- to open-state thin filament transition is known to contribute in part to the activation of muscle thin filaments [1]. In order to ascertain if any of the differences observed in the regulated motility assay can be attributed to differences in the ability of myosin to activate thin filaments containing mutant tropomyosins, we studied the effect of myosin loading concentration on the *in vitro* motility of calcium-regulated thin filaments at submaximal calcium activation levels. While the maximal sliding velocity and fraction motile are similar to that seen at pCa 7 in the pCa curves (Fig. 7 inset), the rate of velocity increase as a function of myosin loading (Fig. 7A) shows no significant differences. This suggests that at the level of detection neither the inhibition nor the enhancement of strong cross-bridge binding to regulated thin filaments is an obvious cause of the mutation-dependent differences in thin filament activation measured (Fig. 6).

Discussion

In this study, we examined two mutations in the human cardiac tropomyosin molecule linked to HCM and DCM. First we assessed their structural impact on tropomyosin coiled-coil behavior and then their corresponding functional influence on thin filament motility and thus on myosin interactions with actin.

Tropomyosin is a stereotypical coiled-coil protein with unique repeating heptad (*a-g*) motifs that determine its super-helical structure [33]. The HCM mutation, E62Q, occurs at an *f* position [20] replacing a charged glutamate residue normally in a favorable position to interact with basic binding partners on actin [12,13]. The E40K mutation, on the other hand, resides at an *e* position in a heptad [18] and is part of the *e-g* paired inter-chain ionic interaction normally facilitating dimeric coiled-coil structural stability and stiffness [19]. Using a combination of computational modeling and *in vitro* motility, we measured structural effects of altered mutant tropomyosin coiled-coils on actin-tropomyosin interaction and then correlated these with functional studies and phenotypical impact.

Consistent with molecular dynamics simulations performed here and previous energy landscape data [14], *in vitro* motility data on E62Q tropomyosin suggests that the mutation disrupts interactions between tropomyosin and actin that normally stabilize the B- thin filament state. Alternatively, E62Q may also destabilize the intermediate closed/C off-state, which we have not directly assessed by our approaches, but which would be consistent with energy landscape measurements [see Fig. 3a in reference 14]. The effects, in turn, will increase the number of motile filaments at low calcium levels and causes less inhibition of motility at low myosin concentrations than elicited by wild-type tropomyosin (Fig. 5 and 6).

The E40K mutation decreases cooperativity of activation (Fig. 6; Table 2), consistent with a reduction in tropomyosin flexural rigidity noted during MD simulations, and evident from the decrease in persistence length (Table 1) as well as the increased local structural flexibility (Fig. 3). Here, the increased flexibility of the mutant parallels subtle molecular rearrangements in the coiled-coil. The disruption of the *e-g* pair between E40 and R35 by the E40K mutation observed during MD, and simultaneous rearrangement of neighboring

pairs, is consistent with this notion. In addition, MD simulation of E40K tropomyosin once bound to actin shows that such rearrangements appear to deform the overall tropomyosin coiled-coil causing global alterations in contacts with actin (Fig. 2), consistent with the stabilization of the B-state and reduced calcium-sensitivity noted in Figure 6.

Our motility data and those of others [34] on the E40K mutant could be explained by a weakening of the open/M-state itself and responsiveness of actin-tropomyosin to strong myosin binding. In turn, this mechanism [34] might indirectly favor an already strengthened blocked-state. Our data provides no obvious direct support for this possibility. In fact, our previous results [14,15] show that the open/M-state binding of wild-type tropomyosin to myosin-free actin already is exceedingly weak. Moreover, residue 40 of tropomyosin does not appear to come into contact with myosin during strong crossbridge binding on F-actin [17], and thus it is not apparent how the mutation could directly impact strong binding without concomitant major conformational changes taking place.

Increased tropomyosin flexibility is frequently considered a hallmark of increased calcium-sensitivity, biasing movement away from the blocked- (or closed-) states. Here, we have found that this “rule of thumb” is likely to be an over-simplification (e.g. see Table 3). Indeed, the E62Q variant, featuring a mutation that leads to enhanced calcium-sensitivity is no more flexible than the control. And in fact, the E40K mutant, which leads to decreased thin filament stiffness, decreases calcium-sensitivity. Evidently the two mutations examined in the current study influence regulatory function by impacting actin-tropomyosin-myosin binding and not by tropomyosin flexibility.

Our results, examining tropomyosin function and the effect of mutations at the single molecule level are consistent with several studies that examined the effects of the E62Q and E40K tropomyosin mutations in skinned fibers [35], myofibrillar samples [36], reconstituted thin filaments [14,34,37], and isolated proteins [36]. The results of the present work extend those previously evinced and demonstrate that disruption of specific contacts within tropomyosin molecules or at the acto-tropomyosin interface can be subtle and involve both local and long-range effects. In turn, these may affect the position of tropomyosin on actin and ultimately alter the inhibitory or activating states of the thin filament. Mutations that either increase or decrease interactions between B-state tropomyosin and actin are generally associated with corresponding decreased or increased calcium-sensitivity (e.g., [38]) and often times mutations that increase calcium-sensitivity parallel a loss of tropomyosin inhibitory function. However, the effects of disease-linked point mutations on contractile protein structure and protein-protein interactions are not always easily predicted directly from sequence considerations. Thus, relationships between mutation type and disease categories are not necessarily obvious. The multi-faceted combination of computational and experimental biochemistry used here allow alterations in thin filament regulation to be understood at a fundamental molecular level. This information can potentially help guide targeted treatment modalities well in advance of compensatory cascades affecting disease presentation.

Supplementary Material

Refer to Web version on PubMed Central for supplementary material.

Acknowledgments

These studies were supported by NIH grants R01HL077280 (to J.R.M.), R01HL123774 (to J.R.M. and W.L.), and R37HL036153 (to W.L.). Our customized 5-node, 140 CPU-Linux cluster at the Massachusetts Green High Performance Computing Center provided dedicated computational resources.

Abbreviations

HCM	hypertrophic cardiomyopathy
DCM	dilated cardiomyopathy
MD	molecular dynamics
Tm	tropomyosin
WT	wildtype

References

1. McKillop DF, Geeves MA. Regulation of the interaction between actin and myosin subfragment 1: evidence for three states of the thin filament. Biophys J. 1993; 65(2):693–701. [PubMed: 8218897]
2. McKillop DF, Geeves MA. Regulation of the acto.myosin subfragment 1 interaction by troponin/tropomyosin. Evidence for control of a specific isomerization between two acto.myosin subfragment 1 states. The Biochemical journal. 1991; 279(Pt 3):711–8. [PubMed: 1953663]
3. Vibert P, Craig R, Lehman W. Steric-model for activation of muscle thin filaments. Journal of molecular biology. 1997; 266(1):8–14. [PubMed: 9054965]
4. Paul DM, Morris EP, Kensler RW, Squire JM. Structure and orientation of troponin in the thin filament. The Journal of biological chemistry. 2009; 284(22):15007–15. [PubMed: 19321455]
5. Galinska-Rakoczy A, Engel P, Xu C, Jung H, Craig R, Tobacman LS, Lehman W. Structural basis for the regulation of muscle contraction by troponin and tropomyosin. Journal of molecular biology. 2008; 379(5):929–35. [PubMed: 18514658]
6. Gomes AV, Potter JD, Szczesna-Cordary D. The role of troponins in muscle contraction. IUBMB Life. 2002; 54(6):323–33. [PubMed: 12665242]
7. Boussouf SE, Geeves MA. Tropomyosin and troponin cooperativity on the thin filament. Advances in experimental medicine and biology. 2007; 592:99–109. [PubMed: 17278359]
8. Lehman W, Hatch V, Korman V, Rosol M, Thomas L, Maytum R, Geeves MA, Van Eyk JE, Tobacman LS, Craig R. Tropomyosin and actin isoforms modulate the localization of tropomyosin strands on actin filaments. Journal of molecular biology. 2000; 302(3):593–606. [PubMed: 10986121]
9. Perz-Edwards RJ, Irving TC, Baumann BA, Gore D, Hutchinson DC, Krzic U, Porter RL, Ward AB, Reedy MK. X-ray diffraction evidence for myosin-troponin connections and tropomyosin movement during stretch activation of insect flight muscle. Proceedings of the National Academy of Sciences of the United States of America. 2011; 108(1):120–5. [PubMed: 21148419]
10. Schmidt WM, Lehman W, Moore JR. Direct observation of tropomyosin binding to actin filaments. Cytoskeleton (Hoboken). 2015; 72(6):292–303. [PubMed: 26033920]
11. Poole KJ, Lorenz M, Evans G, Rosenbaum G, Pirani A, Craig R, Tobacman LS, Lehman W, Holmes KC. A comparison of muscle thin filament models obtained from electron microscopy reconstructions and low-angle X-ray fibre diagrams from non-overlap muscle. J Struct Biol. 2006; 155(2):273–84. [PubMed: 16793285]

12. Li XE, Tobacman LS, Mun JY, Craig R, Fischer S, Lehman W. Tropomyosin position on F-actin revealed by EM reconstruction and computational chemistry. Biophys J. 2011; 100(4):1005–13. [PubMed: 21320445]
13. Orzechowski M, Li XE, Fischer S, Lehman W. An atomic model of the tropomyosin cable on F-actin. Biophys J. 2014; 107(3):694–699. [PubMed: 25099808]
14. Orzechowski M, Fischer S, Moore JR, Lehman W, Farman GP. Energy landscapes reveal the myopathic effects of tropomyosin mutations. Archives of biochemistry and biophysics. 2014; 564:89–99. [PubMed: 25241052]
15. Orzechowski M, Moore JR, Fischer S, Lehman W. Tropomyosin movement on F-actin during muscle activation explained by energy landscapes. Archives of biochemistry and biophysics. 2014; 545:63–8. [PubMed: 24412204]
16. Rynkiewicz MJ, Schott V, Orzechowski M, Lehman W, Fischer S. Electrostatic interaction map reveals a new binding position for tropomyosin on F-actin. J Muscle Res Cell Motil. 2015; 36(6): 525–33. [PubMed: 26286845]
17. Behrmann E, Muller M, Penczek PA, Mannherz HG, Manstein DJ, Raunser S. Structure of the rigor actin-tropomyosin-myosin complex. Cell. 2012; 150(2):327–38. [PubMed: 22817895]
18. Olson TM, Kishimoto NY, Whitby FG, Michels VV. Mutations that alter the surface charge of alpha-tropomyosin are associated with dilated cardiomyopathy. Journal of molecular and cellular cardiology. 2001; 33(4):723–32. [PubMed: 11273725]
19. Brown JH, Kim KH, Jun G, Greenfield NJ, Dominguez R, Volkmann N, Hitchcock-DeGregori SE, Cohen C. Deciphering the design of the tropomyosin molecule. Proceedings of the National Academy of Sciences of the United States of America. 2001; 98(15):8496–501. [PubMed: 11438684]
20. Jongbloed RJ, Marcelis CL, Doevendans PA, Schmeitz-Mulkens JM, Van Dockum WG, Geraedts JP, Smeets HJ. Variable clinical manifestation of a novel missense mutation in the alpha-tropomyosin (TPM1) gene in familial hypertrophic cardiomyopathy. J Am Coll Cardiol. 2003; 41(6):981–6. [PubMed: 12651045]
21. Li XE, Holmes KC, Lehman W, Jung H, Fischer S. The shape and flexibility of tropomyosin coiled coils: implications for actin filament assembly and regulation. Journal of molecular biology. 2010; 395(2):327–39. [PubMed: 19883661]
22. Humphrey W, Dalke A, Schulten K. VMD: visual molecular dynamics. J Mol Graph. 1996; 14(1): 33–8. 27–8. [PubMed: 8744570]
23. Phillips JC, Braun R, Wang W, Gumbart J, Tajkhorshid E, Villa E, Chipot C, Skeel RD, Kale L, Schulten K. Scalable molecular dynamics with NAMD. J Comput Chem. 2005; 26(16):1781–802. [PubMed: 16222654]
24. Brooks BR, Brooks CL 3rd, Mackerell AD Jr, Nilsson L, Petrella RJ, Roux B, Won Y, Archontis G, Bartels C, Boresch S, Caflisch A, Caves L, Cui Q, Dinner AR, Feig M, Fischer S, Gao J, Hodoscek M, Im W, Kuczera K, Lazaridis T, Ma J, Ovchinnikov V, Paci E, Pastor RW, Post CB, Pu JZ, Schaefer M, Tidor B, Venable RM, Woodcock HL, Wu X, Yang W, York DM, Karplus M. CHARMM: the biomolecular simulation program. J Comput Chem. 2009; 30(10):1545–614. [PubMed: 19444816]
25. Li XE, Lehman W, Fischer S. The relationship between curvature, flexibility and persistence length in the tropomyosin coiled-coil. J Struct Biol. 2010; 170(2):313–8. [PubMed: 20117217]
26. Coulton AT, Koka K, Lehrer SS, Geeves MA. Role of the head-to-tail overlap region in smooth and skeletal muscle beta-tropomyosin. Biochemistry. 2008; 47(1):388–97. [PubMed: 18069797]
27. Wannenburg T, Heijne GH, Geerdink JH, Van Den Dool HW, Janssen PM, De PP. Tombe, Cross-bridge kinetics in rat myocardium: effect of sarcomere length and calcium activation. Am J Physiol Heart Circ Physiol. 2000; 279(2):H779–90. [PubMed: 10924078]
28. Veigel C, Schmitz S, Wang F, Sellers JR. Load-dependent kinetics of myosin-V can explain its high processivity. Nat Cell Biol. 2005; 7(9):861–9. [PubMed: 16100513]
29. Moore JR, Krementsova EB, Trybus KM, Warshaw DM. Myosin V exhibits a high duty cycle and large unitary displacement. J Cell Biol. 2001; 155(4):625–35. [PubMed: 11706052]
30. Holmes KC, Lehman W. Gestalt-binding of tropomyosin to actin filaments. J Muscle Res Cell Motil. 2008; 29(6–8):213–9. [PubMed: 19116763]

31. Rynkiewicz MJ, Prum T, Hollenberg S, Kiani FA, Fagnant PM, Marston SB, Trybus KM, Fischer S, Moore JR, Lehman W. Tropomyosin Must Interact Weakly with Actin to Effectively Regulate Thin Filament Function. Biophys J. 2017; 113(11):2444–2451. [PubMed: 29211998]
32. Lehrer SS, Morris EP. Comparison of the effects of smooth and skeletal tropomyosin on skeletal actomyosin subfragment 1 ATPase. The Journal of biological chemistry. 1984; 259(4):2070–2. [PubMed: 6230348]
33. Brown JH, Cohen C. Regulation of muscle contraction by tropomyosin and troponin: how structure illuminates function. Adv Protein Chem. 2005; 71:121–59. [PubMed: 16230111]
34. Mirza M, Robinson P, Kremneva E, Copeland O, Nikolaeva O, Watkins H, Levitsky D, Redwood C, El-Mezgueldi M, Marston S. The effect of mutations in alpha-tropomyosin (E40K and E54K) that cause familial dilated cardiomyopathy on the regulatory mechanism of cardiac muscle thin filaments. The Journal of biological chemistry. 2007; 282(18):13487–97. [PubMed: 17360712]
35. Bai F, Groth HL, Kawai M. DCM-related tropomyosin mutants E40K/E54K over-inhibit the actomyosin interaction and lead to a decrease in the number of cycling cross-bridges. PLoS One. 2012; 7(10):e47471. [PubMed: 23077624]
36. Chang AN, Potter JD. Sarcomeric protein mutations in dilated cardiomyopathy. Heart Fail Rev. 2005; 10(3):225–35. [PubMed: 16416045]
37. Gupte TM, Haque F, Gangadharan B, Sunitha MS, Mukherjee S, Anandhan S, Rani DS, Mukundan N, Jambekar A, Thangaraj K, Sowdhamini R, Sommese RF, Nag S, Spudich JA, Mercer JA. Mechanistic heterogeneity in contractile properties of alpha-tropomyosin (TPM1) mutants associated with inherited cardiomyopathies. The Journal of biological chemistry. 2015; 290(11): 7003–15. [PubMed: 25548289]
38. Donkervoort S, Papadaki M, de Winter JM, Neu MB, Kirschner J, Bolduc V, Yang ML, Gibbons MA, Hu Y, Dastgir J, Leach ME, Rutkowski A, Foley AR, Kruger M, Wartchow EP, McNamara E, Ong R, Nowak KJ, Laing NG, Clarke NF, Ottenheijm C, Marston SB, Bonnemann CG. TPM3 deletions cause a hypercontractile congenital muscle stiffness phenotype. Ann Neurol. 2015; 78(6):982–994. [PubMed: 26418456]
39. Moore JR, Li X, Nirody J, Fischer S, Lehman W. Structural implications of conserved aspartate residues located in tropomyosin's coiled-coil core. Bioarchitecture. 2011; 1(5):250–255. [PubMed: 22754618]
40. Sumida JP, Wu E, Lehrer SS. Conserved Asp-137 imparts flexibility to tropomyosin and affects function. The Journal of biological chemistry. 2008; 283(11):6728–34. [PubMed: 18165684]
41. Shchepkin DV, Matyushenko AM, Kopylova GV, Artemova NV, Bershitsky SY, Tsaturyan AK, Levitsky DI. Stabilization of the Central Part of Tropomyosin Molecule Alters the Ca2+-sensitivity of Actin-Myosin Interaction. Acta Naturae. 2013; 5(3):126–9. [PubMed: 24303208]
42. Li XE, Suphamungmee W, Janco M, Geeves MA, Marston SB, Fischer S, Lehman W. The flexibility of two tropomyosin mutants, D175N and E180G, that cause hypertrophic cardiomyopathy. Biochem Biophys Res Commun. 2012; 424(3):493–6. [PubMed: 22789852]
43. Loong CK, Zhou HX, Chase PB. Familial hypertrophic cardiomyopathy related E180G mutation increases flexibility of human cardiac alpha-tropomyosin. FEBS Lett. 2012; 586(19):3503–7. [PubMed: 22958892]
44. Bing W, Knott A, Redwood C, Esposito G, Purcell I, Watkins H, Marston S. Effect of hypertrophic cardiomyopathy mutations in human cardiac muscle alpha-tropomyosin (Asp175Asn and Glu180Gly) on the regulatory properties of human cardiac troponin determined by in vitro motility assay. Journal of molecular and cellular cardiology. 2000; 32(8):1489–98. [PubMed: 10900175]
45. Ly S, Lehrer SS. Long-range effects of familial hypertrophic cardiomyopathy mutations E180G and D175N on the properties of tropomyosin. Biochemistry. 2012; 51(32):6413–20. [PubMed: 22794249]
46. Lehman W, Medlock G, Li XE, Suphamungmee W, Tu AY, Schmidtmann A, Ujfalusi Z, Fischer S, Moore JR, Geeves MA, Regnier M. Phosphorylation of Ser283 enhances the stiffness of the tropomyosin head-to-tail overlap domain. Archives of biochemistry and biophysics. 2015; 571:10–5. [PubMed: 25726728]

47. Heeley DH, Watson MH, Mak AS, Dubord P, Smillie LB. Effect of phosphorylation on the interaction and functional properties of rabbit striated muscle alpha alpha-tropomyosin. The Journal of biological chemistry. 1989; 264(5):2424–30. [PubMed: 2521628]

48. Rao VS, Marongelli EN, Guilford WH. Phosphorylation of tropomyosin extends cooperative binding of myosin beyond a single regulatory unit. Cell Motil Cytoskeleton. 2009; 66(1):10–23. [PubMed: 18985725]

49. Sewanan LR, Moore JR, Lehman W, Campbell SG. Predicting Effects of Tropomyosin Mutations on Cardiac Muscle Contraction through Myofilament Modeling. Front Physiol. 2016; 7:473. [PubMed: 27833562]

50. Sousa D, Cammarato A, Jang K, Graceffa P, Tobacman LS, Li XE, Lehman W. Electron microscopy and persistence length analysis of semi-rigid smooth muscle tropomyosin strands. Biophys J. 2010; 99(3):862–8. [PubMed: 20682264]

51. Hagemann UB, Mason JM, Muller KM, Arndt KM. Selectional and mutational scope of peptides sequestering the Jun-Fos coiled-coil domain. Journal of molecular biology. 2008; 381(1):73–88. [PubMed: 18586270]

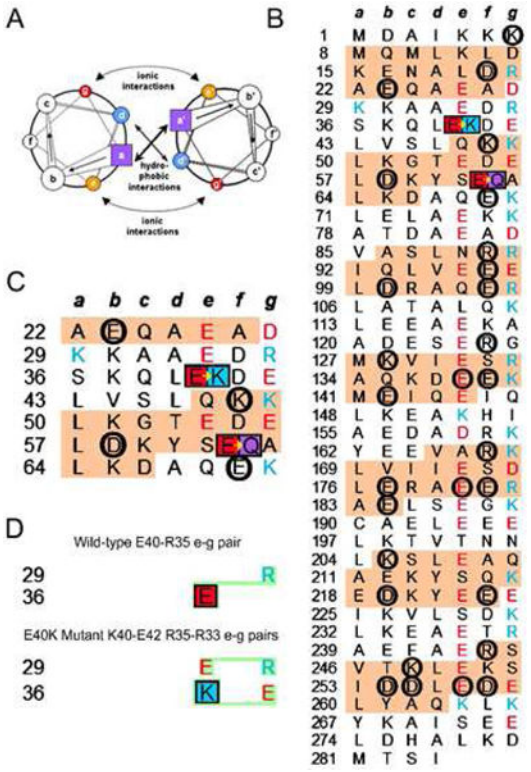

Figure 1. Tropomyosin is a canonical coiled-coil

A. Helical wheel diagram of a canonical dimeric coiled-coil. Heptad positions are labeled *a* to *g* and *a′* to *g′* for the respective helices of such a dimer. Figure adapted from [51]. B. Striated muscle tropomyosin (Tpm1.1) sequence annotation. Figure adapted and modified from references [14,19,33] to emphasize residues within heptad repeats (*a, b, c, d, e, f, g*) in each chain of the tropomyosin coiled-coil homodimer, with the first residue in each heptad repeat numbered. The so-called α-zones of each pseudo-repeat of tropomyosin [33] that locate close to actin subdomains 1 and 3 are shaded in tan (β-zones found over subdomains 2 and 4 are white). The α-zones contain most of the amino acid residues (circled) that interact electrostatically with oppositely charged residues on actin [12,14]. Acidic and basic amino acids that form *e-g* pairs are highlighted in red and blue; residue 29, a non-canonical charged residue at an *a*-position may also interact with a neighboring *e-g* pair. Black boxes mark mutations in tropomyosin (E40K and E62Q) that have been investigated in the current study. C. Enlargement of B showing α-and β-zones of tropomyosin, which contain these mutations. Note that in wild-type tropomyosin *f*-position E62 participates in actin-binding, while *e*-position E40 is part of an *e-g* pair. D. New *e-g* pairing resulting from E40K mutation.

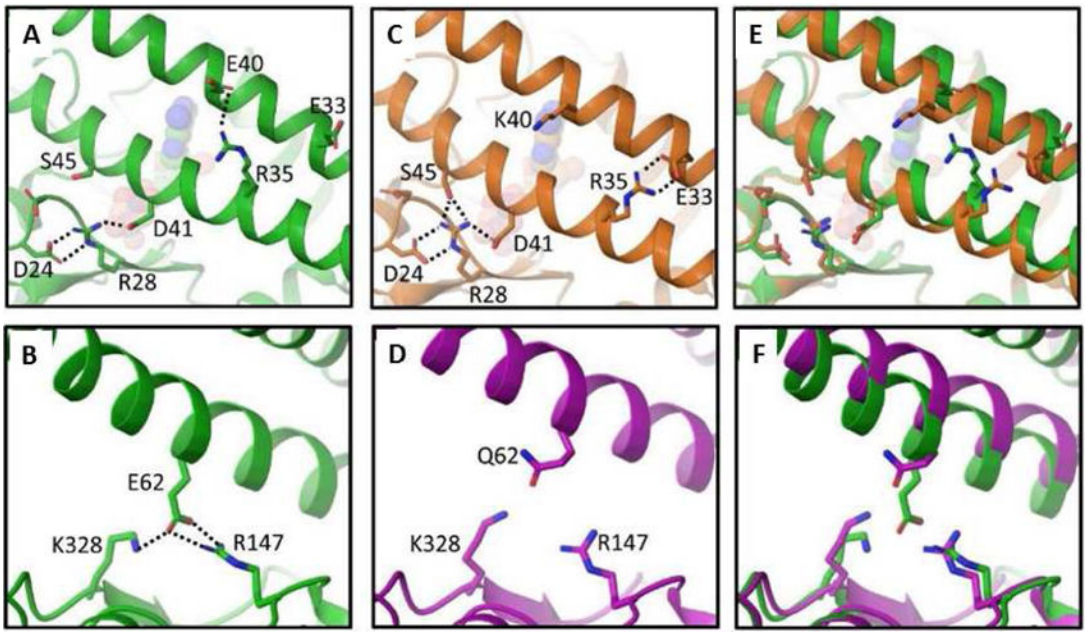

Figure 2.

Molecular dynamics simulations were used to assess the impact of DCM mutant (E40K; Panels A, C, E) and HCM mutant (E62Q; Panels B, D, & F) on the distance between tropomyosin and actin. Introducing lysine at position 40 in the E40K mutant (Panels C, E) causes a shift in the tropomyosin allowing Ser45 of tropomyosin to swing in and make a contact with Arg28 of actin. This mutation also forces Arg35 on tropomyosin to rotate, allowing it to interact with Glu33 of the opposite chain. New pairing of Lys48 of tropomyosin and Asp25 of actin occurs sporadically (not shown). These altered interactions cause one chain of tropomyosin to move closer to the actin, causing a slight separation from the second chain (Panel E). At the same time, the HCM mutation (Panels D, F) eliminates the interaction of tropomyosin at position 62 with the two positively charged actin residues at positions 147 and 328, resulting in tropomyosin movement away from the actin surface during MD (Panel F).

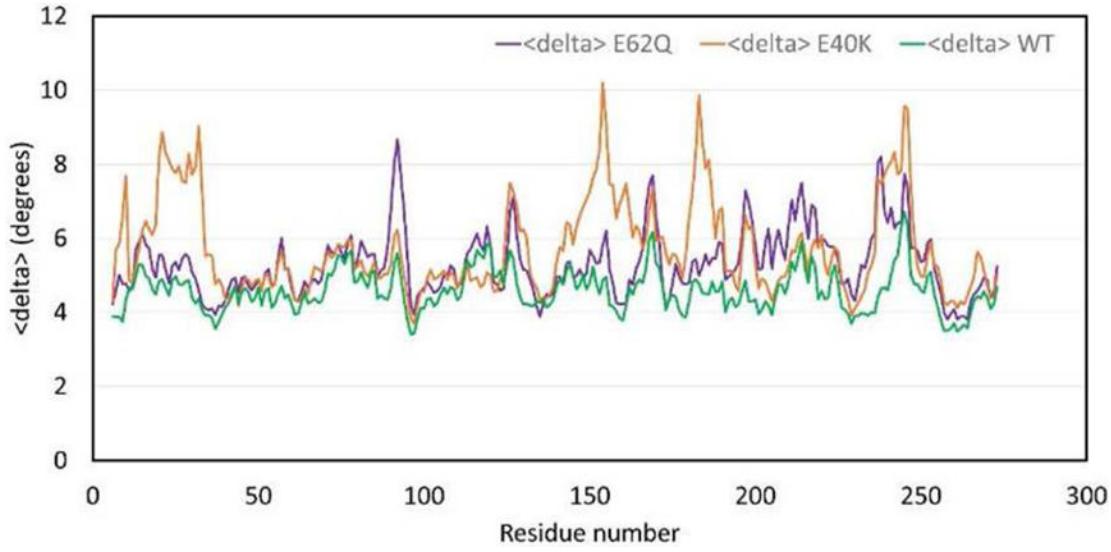

Figure 3.

Local changes in tropomyosin flexibility induced by the disease-linked mutations E40K (gold) and E62Q (purple) compared to wild-type (green). Local flexibility is determined as the time average of the local angular deviations from the average structure. The E40K tropomyosin shows increased flexibility in the N-terminal direction away from the mutation site as well as delocalized effects in the C-terminal half of the molecule. The E62Q mutation shows minimal effects on local flexibility.

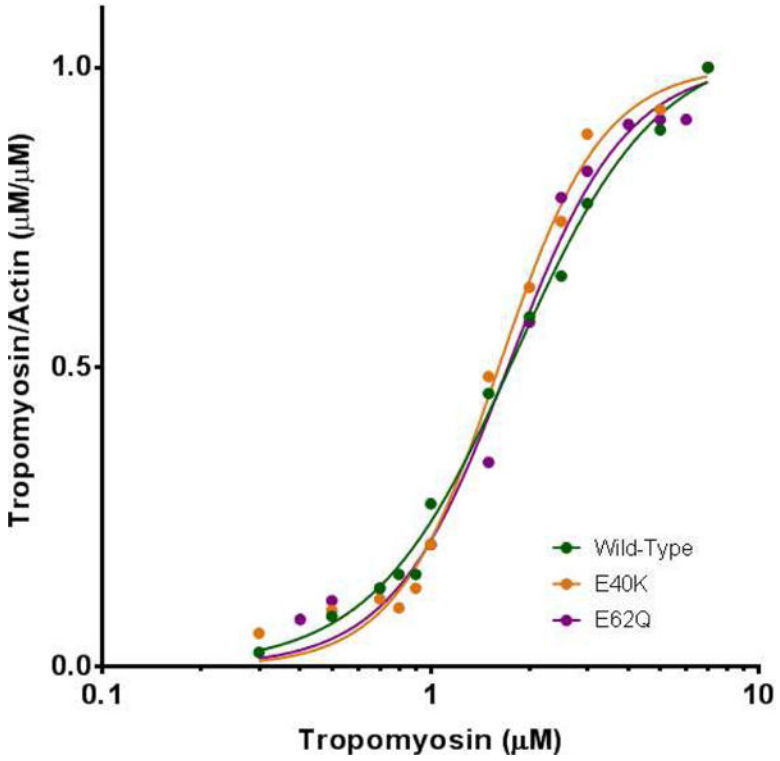

Figure 4. Mutant and wild-type tropomyosin binding to F-actin

Several concentrations (0.3–7 μM) were incubated with 1 μM F-actin. Bound tropomyosin was determined by sedimentation at 100,000 × g in an Airfuge (Beckman-Coulter; Brea, CA) and plotted against added free tropomyosin. Fractional saturation of F-actin by mutant tropomyosin in pellets was calculated from the relative band densities of 12% SDS-PAGE gels using ImageJ software. Bound tropomyosin was plotted for wild-type (green circles), E40K (gold circles) and E62Q tropomyosin (purple circles). Data were fit to the Hill-type binding equation $Y=B_{max}*[Tm]^h/(Kd^h + [Tm]^h)$ using GraphPad Prism 7.04 Software. Apparent binding affinities of mutant tropomyosins were similar to wild-type (K_d ± SEM: 1.8 ± 0.1μM, 1.6 ± 0.07 μM, 1.7 ± 0.1 μM and *h*: 2.0 ± 0.14, 2.7 ± 0.23, 2.43 ± 0.11 for wild-type, E40K, and E62Q respectively).

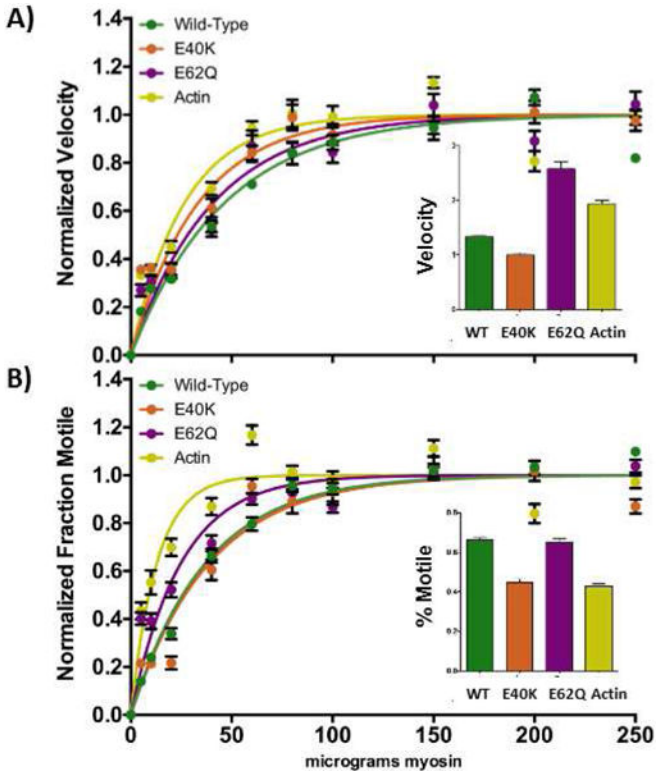

Figure 5. Impact of myosin concentration on troponin-free actin sliding velocity

Myosin-dependent changes in troponin-free actin filament sliding (Panel A) show differences in velocities of actin containing wild-type tropomyosin (green) and E40K mutant tropomyosin (gold) and tropomyosin-free actin filaments (yellow). However, the myosin-dependent changes in velocity for the E62Q mutant (purple) was not different from wild-type even though the maximal sliding velocity was larger (inset). Panel B shows the impact of tropomyosin on the fraction of motile filaments. Unlike the velocity relationship, the DCM mutant E40K tropomyosin showed no difference in the myosin dependence of motile filaments when compared to wild-type while actin associated with E62Q-mutant tropomyosin required less myosin to reach maximal velocity. Examining the maximal fraction of motile filaments as a function of tropomyosin variants, (inset Panel B) shows that values for both the DCM mutant and bare actin were lower than wild-type or the HCM mutant; the latter were not significantly different from each other. Each point represents the average and error bars represent the SEM.

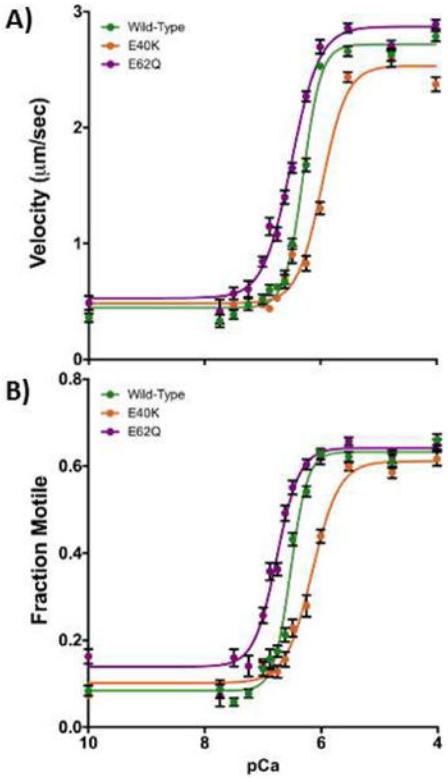

Figure 6. Impact of mutant tropomyosin on calcium-regulated filaments

Velocity/pCa relationships of actin filaments containing either wild-type (green), E40K (gold), or E62Q (purple) tropomyosin. Panel A shows that introduction of mutant tropomyosin either increased calcium-sensitivity, when HCM mutant E62Q tropomyosin was added, or decreased velocity and calcium-sensitivity, when DCM mutant E40K tropomyosin was added. Examining the impact of these mutations on the fraction motile filaments (Panel B), showed that the DCM and HCM mutants had a similar effect on calcium-sensitivity as observed for velocity measurements, with the HCM mutation showing an increased fraction motile at lower calcium levels, indicating impaired blocked- or closed-state interaction between actin and tropomyosin. Each point represents the average and error bars represent the SEM; again differences noted are significant at P values greater than 99%. The Hill equation describing the pCa-velocity relationship was then fitted to these data and plotted as a color coded solid line.

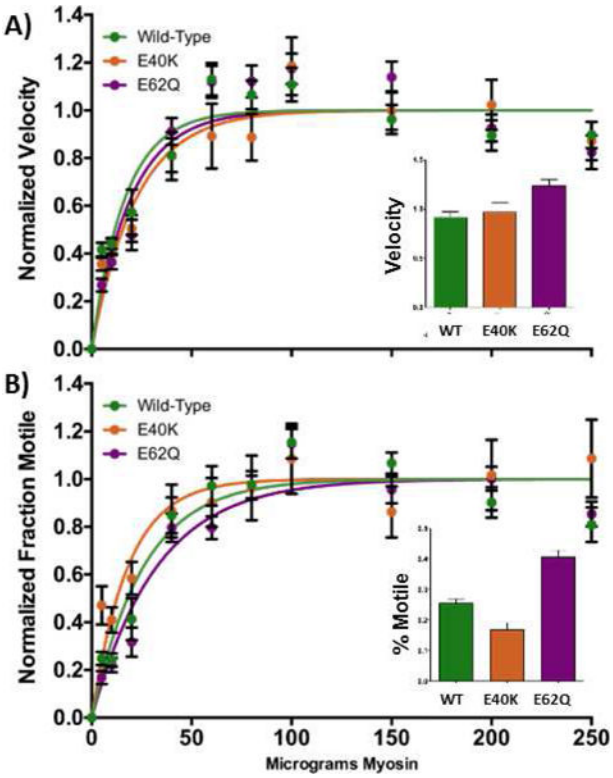

Figure 7. Impact of varied myosin concentration on troponin-regulated actin sliding velocity at pCa 7

While the maximal sliding velocity and fraction motile for the wild-type and mutants (inset panels A, Velocity, and B, Fraction Motile) were similar to observations in Figure 5, there was no significant difference in the myosin-dependent activation of velocity and fraction motile. This indicates that myosin-dependent changes in velocity are not generally altered by the introduction of the mutations at E62 and E40 when troponin is present. Each point represents the average and error bars SEM.

Table 1

Persistence length measurements of tropomyosin mutants. The relatively high PL_a and low PL_d for E40K for this mutant indicates that it is straighter and more flexible than wild-type and E62Q tropomyosin.

	Apparent Persistence Length (PL_a)	**Dynamic Persistence Length (PL_d)**
WT	93 nm	479 nm
E62Q	91 nm	456 nm
E40K	122 nm	219 nm

Table 2

Calculated pCa_{50} and Hill coefficients (n_H) for the actin sliding velocity and fraction motile from the data in Figure 6 for all three tropomyosin constructs examined, SEM represent errors.

Tropomyosin	Velocity pCa_{50}	Velocity Hill coefficient n_H	Fraction Motile pCa_{50}	Fraction Motile Hill coef. n_H
WT	6.3±0.03	2.0±0.15	6.5±0.04	2.3±0.25
E40K	5.9±0.06	1.4±0.13	6.1±0.06	1.3±0.13
E62Q	6.5±0.04	1.5±0.13	6.8±0.03	2.4±0.32

Table 3

Tropomyosin flexibility is not a reliable predictor for calcium sensitivity.

Tropomyosin Mutation	Effect on Tropomyosin Flexibility	Effect on Calcium-Sensitivity
A74L/A78V/A81 L[21]	↑	Not known
C190A/D137L[39–41]	↓	↑
E180G[42–45]	↑	↑
D175N[42, 44, 45]	↑	↑
S282D[46–48]	↓	↑
E192K[49]	↑	↑
E62Q *	none observed	↑
E40K *	↑	↓

A variety of techniques have been used to determine flexibility of tropomyosin mutants, including persistence length measurements on tropomyosin molecules following molecular dynamics simulations [12,21,25,39,42,46,49], by electron microscopy of rotary shadowed and negatively stained samples [21,25,42,50] and by atomic force microscopy [43]. Note that local stiffness increased in the surrounds of the C190A/D137L mutation, but global stiffness over the entire molecule decreased[39].

* results from this paper.